ACS APPLIED MATERIALS & INTERFACES

Research Article

www.acsami.org

Two-Step Electrochemical Synthesis of Polypyrrole/Reduced Graphene Oxide Composites as Efficient Pt-Free Counter Electrode for Plastic Dye-Sensitized Solar Cells

Wantao Liu,[†,‡] Yanyan Fang,[§] Peng Xu,[‡] Yuan Lin,[§] Xiong Yin,*[,‡] Guangshi Tang,*[,†] and Meng He*[,‡]

[†]Department of Chemistry, School of Science, Beijing University of Chemical Technology, Beijing 100029, P. R. China

[‡]National Center for Nanoscience and Technology, Beijing 100190, P. R. China

[§]Key Laboratory of Photochemistry, Beijing National Laboratory for Molecular Sciences (BNLMS), Institute of Chemistry, Chinese Academy of Sciences, Beijing 100190, P. R. China

Supporting Information

ABSTRACT: Polypyrrole/reduced graphene oxide (PPy/RGO) composites on the rigid and plastic conducting substrates were fabricated via a facile two-step electrochemical process at low temperature. The polypyrrole/graphene oxide (PPy/GO) composites were first prepared on the substrate with electrochemical polymerization method, and the PPy/RGO composites were subsequently obtained by electrochemically reducing the PPy/GO. The resultant PPy/GO and PPy/RGO composites were porous, in contrast to the dense and flat pristine PPy films. The cyclic voltammetry measurement revealed that resultant composites exhibited a superior catalytic performance for triiodide reduction in the order of PPy/RGO > PPy/GO > PPy. The catalytic activity of PPy/RGO was comparable to that of Pt counter electrode (CE). Under the optimal conditions, an energy conversion efficiency of 6.45% was obtained for a rigid PPy/RGO-based dye-sensitized solar cell, which is 90% of that for a thermally deposited Pt-based device (7.14%). A plastic counter electrode was fabricated by depositing PPy/RGO composites on the plastic ITO/PEN substrate, and then an all-plastic device was assembled and exhibited an energy conversion efficiency of 4.25%, comparable to that of the counterpart using a sputtered-Pt CE (4.83%) on a plastic substrate. These results demonstrated that electrochemical synthesis is a facile low-temperature method to fabricate high-performance RGO/polymer composite-based CEs for plastic DSCs.

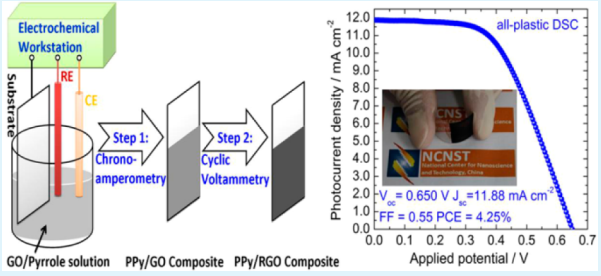

KEYWORDS: *dye-sensitized solar cells, polypyrrole, reduced graphene oxide, plastic substrate, electrochemical polymerization, composites, low-temperature fabrication, Pt-free*

INTRODUCTION

Dye-sensitized solar cells (DSCs) have been attracting widespread attention because of their low cost, simple fabrication process, and relatively high energy conversion efficiency.[1−3] A typical dye-sensitized solar cell is composed of dye-absorbed photoanode, liquid electrolyte and counter electrode (CE).[1] As energy conversion efficiency depends on the redox reaction at the electrolyte/CE interfaces, counter electrode would play an important role in reducing the oxidized species, and thus determining the conversion efficiency.[4,5] The traditional material for CE in DSCs is Pt metal due to its high conductivity and excellent catalytic ability for triiodide reduction.[4] However, its corrosion from triiodide contained in the electrolyte and its high-cost limit its application in large-scale manufacture and long-term running.[4,5] Lots of efforts have been devoted to developing new alternative materials for counter electrode. Conductive polymers (CP), such as polypyrrole (PPy),[6−9] polyaniline (PANI)[10,11] and poly(3,4-ethylenedioxythiophene) (PEDOT),[12−15] have been successfully deposited on the FTO or ITO substrates as CEs in DSCs. Meanwhile, carbonaceous materials, including carbon black,[16] carbon tube,[17,18] graphene[19−21] and reduced graphene oxide (RGO),[22−24] were also introduced to replace Pt metal in DSCs.

As a type of functional conductive polymers, PPy has been widely investigated for decades due to its easy preparation, high electrical conductivity and large surface area.[25,26] According to previous reports, the as-fabricated PPy CE showed a relatively low catalytic activity for triiodide reduction in DSC, compared to PANI or PEDOT CEs.[8] One alternative method to enhance its photovoltaic performance is to form composites with suitable materials.[6]

With large specific surface area and super mechanical property, RGO demonstrates promising applications in photoelectrochemical devices.[21,27,28] Recently, RGO, serving as CE in DSCs, has showed excellent catalytic performance on reduction of triiodide, manifesting its potential for substituting Pt metal.

Received: July 8, 2014
Accepted: August 27, 2014
Published: August 27, 2014

Further studies revealed that the catalytic activity for triiodide reduction could be ascribed to the defects and oxygen-containing groups contained in RGO[19−21] Nevertheless, RGO sheets tended to aggregate with each other because of $\pi-\pi$ stacking, and the aggregation would deteriorate the catalytic performance.[21,29] To avoid aggregation, RGO with 3D-structures and RGO-based composites were applied as CEs for DSCs.[30−32] Graphene-quantum-dots (GQDs) doped PPy films were synthesized with electrochemical oxidation deposition method and used as CEs for DSCs.[31] The GQDs in the composite film indeed enhanced the catalytic performance on the triiodide reduction. However, the fill factor and power conversion efficiency of device should be further improved. CEs based on PPy/RGO composites were also reported, and showed an enhanced catalytic performance on the triiodide reduction, in comparison with PPy and RGO CEs.[32] It was worth noting that the PPy/RGO composite was prepared via multiple-step process and highly toxic and dangerous chemical (hydrazine hydrate) was used to reduce the GO to RGO. Electrochemical reduction of GO is a promising choice for RGO preparation, which is an efficient, environmental-friendly and easily controlled method.[28]

In the present work, we report a facile two-step electrochemical process to fabricate PPy/RGO composites on FTO and ITO substrate at low temperature. In the first step, the PPy/GO composites were obtained by electrochemical oxidative polymerization. Graphene oxide (GO) sheets served as weak dopants due to the abundant negative charges on the surfaces, which could be dispersed in the PPy matrix during the electrochemical polymerization process. In the second step, the GO contained in the PPy/GO composites was effectively reduced to RGO through cyclic voltammetry method to obtain PPy/RGO composites. Besides, the whole preparation process of PPy/RGO was performed at low temperature, enabling the application to the plastic substrate. Rigid and plastic DSCs using PPy/RGO composites as CEs showed power conversion efficiencies of 6.45% and 4.25%, respectively, which are comparable to those of their counterparts using Pt CEs. These results indicate that the as-prepared PPy/RGO composite is a promising alternative material to Pt metal to be used as CEs for DSCs.

EXPERIMENTAL SECTION

Materials. Pyrrole was obtained from Aladdin Industrial Inc. Prior to usage, pyrrole was redistilled. Graphite was bought from Alfa Aesar. Sulfuric acid, $KMnO_4$, H_2O_2 (30%) was supplied by Sinopharm Chemical Reagent Co. Ltd. These chemicals and solvents were used as received. All solutions were prepared with deionized water.

Synthesis of PPy/GO Composites on the Substrate. The preparation of GO was carried out using a modified Hummers' method according to previous reports.[33] Electrochemical polymerization of pyrrole was conducted with a rigid FTO or ITO as working electrode, a Pt wire as counter electrode and a Ag/AgCl electrode as reference electrode. All the electrochemical experiments were performed at room temperature in GO aqueous solution (1 mg mL^{-1}) containing 0.1 mol L^{-1} pyrrole, which was saturated with nitrogen gas prior to polymerization. The aqueous solution was ultrasonicated for 30 min to form a uniform solution. PPy/GO-100s, PPy/GO-150s, PPy/GO-200s, and PPy/GO-250s represented the composites prepared with the polymerization time of 100, 150, 200, and 250 s, respectively.

Preparation of PPy/RGO Composites Counter Electrode. The PPy/RGO composites were obtained by cyclic voltammetry (CV) in N_2-saturated Na_2SO_4 aqueous solution (0.5 M) at a scan rate of 50 mV s^{-1} between 0 and −1 V for 10 cycles. The CV was carried out on a potentiostat (CHI660E, CHI instruments) with PPy/GO as working electrode, a Pt wire as counter electrode, a Ag/AgCl electrode as reference electrode. PPy/RGO-100s, PPy/RGO-150s, PPy/RGO-200s, and PPy/RGO-250s represented the samples prepared by electrochemically reducing the corresponding PPy/GO composites, respectively. For comparison, the Pt/FTO CE electrode was prepared by thermal decomposition of H_2PtCl_6 (30 mM in isopropanol) on the rigid FTO and sintered at 385 °C for 30 min.

Fabrication of DSC Devices. TiO_2 photoanodes were fabricated on the FTO glass by doctor-blading technique to obtain a 12 μm TiO_2 layer and a 4 μm thick scattering layer according to previous reports.[1] Subsequently, the TiO_2 electrodes were treated in 40 mM $TiCl_4$ at 70 °C for 30 min, and then, sintered at 450 °C for 30 min. After the temperature dropped to 85 °C, the electrodes were immersed into 0.3 mM N719 dye solution (mixture of acetonitrile and tertiary butanol with volume ratio 1:1) for 18 h. The dye-sensitized TiO_2 film and the CE were separated by a hot-melt Surlyn film (25 μm thick) and liquid electrolyte. The liquid electrolyte was composed of 0.1 mol L^{-1} iodine, 0.6 mol L^{-1} methylhexylimidazolium iodide, 0.5 mol L^{-1} *tert*-butylpyridine, and 0.1 mol L^{-1} lithium iodide in 3-methoxypropionitrile. The plastic TiO_2 electrode was prepared using electrophoretic deposition technique. A pair of plastic PEN-ITO substrates (Kintec, 20 Ω sq^{-1}) was vertically immersed in the P25 TiO_2 suspension and then a 1.6 V cm^{-1} DC field was applied. After that, the as-prepared TiO_2 electrode was heated at 90 °C on a hot plate for 1.5 h to remove the organic solvents. After cooled to room temperature, the as-prepared TiO_2 electrode was further pressed at 10 MPa for 5 min to yield pressed P25 TiO_2 electrode using a manual hydraulic press at room temperature.

Characterization and Measurement. The morphology of the samples was characterized with a field emission scanning electron microscope (FESEM, Hitachi S-4800) and a transmission electron microscope (TEM, FEI Tecnai F20 G^2 U-twin). X-ray photoelectron spectroscopy (XPS) measurements were carried out with an ESCA Lab 250xi spectrometer using Al Kα (1486.6 eV) irradiation as X-ray source. All the spectra were calibrated to the binding energy of the adventitious C 1s peak at 284.8 eV. Raman spectra were recorded using a Renishaw inVia spectrometer under an excitation of the 514 nm laser.

The catalytic activity of Pt, PPy, PPy/GO and PPy/RGO on the triidodide reduction was characterized with CV measurement. The CV measurement was carried out on a potentiostat (CHI660E, CHI instruments) by using the PPy, PPy/GO, PPy/RGO, and Pt as working electrode with working area of 1 cm^2, a Pt wire as counter electrode, a Ag/AgCl electrode as reference electrode, respectively. The scanning was performed at rate of 50 mV s^{-1} in an acetonitrile solution containing $LiClO_4$ (0.1 mol L^{-1}), LiI (10 mmol L^{-1}), and I_2 (1 mmol L^{-1}). The photocurrent density−voltage characteristics of the DSCs were measured under AM 1.5G illumination (100 mW cm^{-2}) using a solar simulator (Oriel Newport) equipped with a 150 W xenon lamp and a digital source meter (2420, Keithley Instruments, USA). The effective irradiated area was 0.2 cm^2. Electrochemical impedance spectroscopy (EIS) measurement was carried out using a frequency response analyzer (Solartron SI 1270) and a potentiostat (Solartron 1287) at amplitude of 10 mV and the open-circuit voltage under light irradiation of 100 mW cm^{-2} in the frequency range from 0.05 to 10^5 Hz. The EIS data was fitted using ZView software.

RESULTS AND DISCUSSION

The PPy/GO composite was deposited on the substrate surface using potentiostatic technique at a constant potential of 0.8 V. The typical current−time curve is shown in Supporting Information Figure S1a. Increased oxidation currents were observed with the deposition time, indicating that the electrochemical polymerization of pyrrole occurred on the substrate. And the oxidation current tended to reach a saturated value, indicating that the electropolymerization reached the balance. The electro-polymerization of pyrrole was also

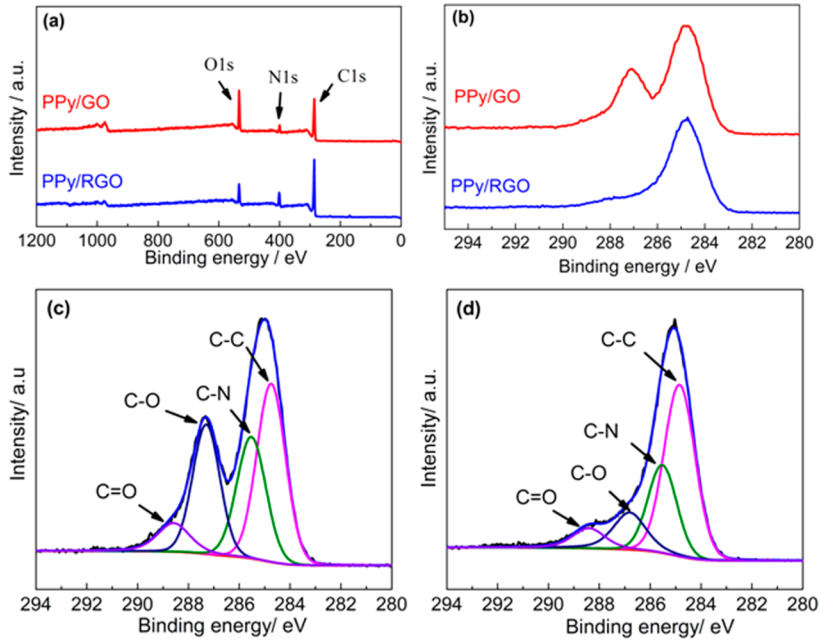

Figure 1. (a) Representative XPS spectra and (b) XPS core level spectra of C 1s for PPy/GO and PPy/RGO composites. The profile fitting of the core level spectra of C 1s for PPy/GO (c) and PPy/RGO (d) composites. The black curves in panels c and d are experimental data, while the blue lines depict the sum of the four disintegrated peaks. The black curves are nearly invisible because of the superimposition of blue lines.

conducted as a control experiment with its current density-time curve shown in Supporting Information Figure S1b. The difference between these two curves indicates that components contained in the solution can affect the electro-polymerization behaviors. In the mixture solution of pyrrole and GO, GO could serve as dopant during the polymerization process, resulting in the formation of PPy/GO composite. GO contained in the PPy/GO composite was further reduced to obtain the PPy/RGO composite. The reduction was performed by cyclic voltammetry (CV) with ten cycles of scanning in the potential range from 0.0 to −1.0 V. It can be seen that a reduction peak appeared at about −0.75 V in CV responses at the first scan (Supporting Information Figure S1c), which is in accordance with previous reports.[34,35] However, no more reduction peak is found in the subsequent scans, which indicates that the electrochemical reduction of GO is an irreversible process. Therefore, GO in the PPy/GO composite was successfully reduced to RGO after the first cycle of scanning. The reduction peak obtained at the first scan could be attributed to the reduction of the oxygen-containing groups, such as −OH and −COOH contained in the PPy/GO composite.

The electrochemical reduction of GO in the PPy/RGO composite was further confirmed by X-ray photoelectron spectroscopy (XPS) analysis. Shown in Figure 1a is the whole XPS spectrum for PPy/GO and PPy/RGO composites. N, O and C were detected in both samples while the intensity ratio of signals from these elements varied significantly. The ratio of C/O of PPy/GO is determined to be 0.9, while that of PPy/RGO is found to be 1.79, indicating effective reduction of oxygen-containing groups in the PPy/GO by electrochemical technique (CV). The C 1s core level XPS spectra of PPy/GO and PPy/RGO are shown in Figure 1b. Two strong peaks were observed for PPy/GO. The peak located at 286.9 eV was interpreted as characteristic signal of oxygenated carbon, and the other one with higher intensity centered at 284.6 eV was attributed to sp^2-carbon.[34−36] The C 1s peaks of PPy/GO and PPy/RGO can be disintegrated into four peaks located at 284.7 (C−C), 285.5 (C−N), 286.8 (C−O) and 288.4 eV (C═O), respectively, and the fitted spectra are presented in Figure 1c and d.[34] In contrast to PPy/GO, PPy/RGO shows only one strong peak around 284.6 eV (C−C). The significant decrease in intensity of the peak at 286.9 eV(C−O) indicates the reduction of GO during the electrochemical reduction process. It demonstrates that oxygen-containing groups in GO were effectively removed and sp^2-carbon was restored after electrochemical reduction. However, there is still a small shoulder peak in the range of 287 and 289 eV, indicating that a fraction of oxygen-containing group (C═O and C−O) was present in the PPy/RGO composite.[34]

The morphology of PPy/GO, PPy/RGO, and PPy films were characterized using SEM. The PPy/GO composite presents a porous surface morphology composed of platelet-like nanostructures (Figure 2a), whereas the PPy film has a quite dense structure (Figure 2c). The morphology of PPy/RGO composite (Figure 2b) changed little in comparison to the PPy/GO composite. The corresponding partially enlarged SEM images for PPy/GO and PPy/RGO composites are shown in Figure 2d and e, respectively. As revealed by SEM observations, the aggregation of GO because of $\pi-\pi$ stacking was strongly suppressed during the electro-polymerization, and the porous morphology of PPy/GO composite was well retained in the subsequent electrochemical reduction process, which is believed to benefit triiodide reduction. One typical cross-sectional SEM image of PPy/RGO composite is shown in Figure 2f. The estimated thickness for PPy/RGO film prepared with deposition time of 100, 150, 200, and 250 s is about 150, 500, 600, and 700 nm, respectively. TEM observation was also performed and images of PPy and PPy/RGO samples were presented in Supporting Information Figure S2.

The catalytic activities for resultant composites toward triiodide reduction process were evaluated with CV using a

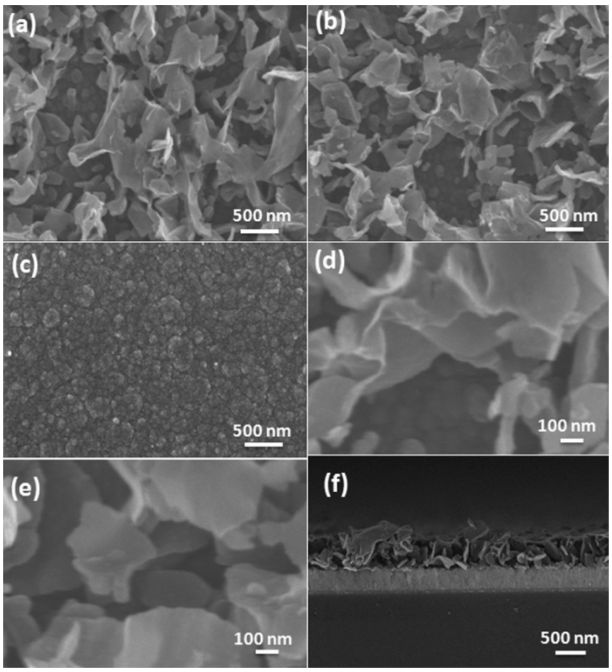

Figure 2. SEM images of the (a, d) PPy/GO, (b, e) PPy/RGO composites, and (c) PPy on FTO substrates and (f) cross-sectional SEM image of PPy/RGO prepared with the deposition time of 150 s.

three-electrode system.[4] And the corresponding CV curves are shown in Figure 3. Two pairs of redox peaks are observed for all electrodes, and they can be assigned to the following two reactions according to previous reports[15,30]

$$3I^- - 2e \leftrightarrow I_3^- \quad (1)$$

$$2I_3^- - 2e \leftrightarrow 3I_2 \quad (2)$$

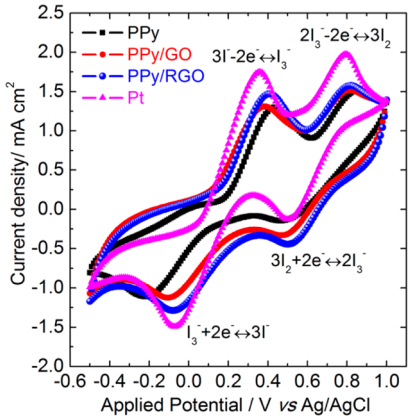

Figure 3. Cyclic voltammograms for PPy, PPy/GO, PPy/RGO, and Pt electrode at a scan rate of 50 mV s^{-1} in acetonitrile solution containing 10 mM LiI, 1 mM I_2, and 0.1 M $LiClO_4$ with a platinum wire and a Ag/AgCl electrode used as counter electrode and reference electrode, respectively.

It is well-known that the redox pair at relatively negative potentials is attributed to reaction 1, whereas the redox pair at the much more positive potentials is assigned to the redox reaction 2. The triiodide ions have to be effectively reduced on the surfaces of CE during the DSC operation. Hence, the negative redox pair (reaction 1) is the research focus of CV analysis. As shown in Figure 3, the separation of cathodic and anodic peaks potential (ΔE_p) for pristine PPy electrode is 0.65 V, whereas, PPy/GO and PPy-RGO composites have an approximately equal value of 0.48 V. The value of ΔE_p for Pt electrode is 0.43 V. ΔE_p decreased after incorporating GO or RGO into the polymer, indicating that triiodide ions were reduced more readily on the composite electrodes than on the pristine polymer electrode.[18,30] In addition, the current density of reduction peak for the different electrodes increases in the order of PPy < PPy/GO < PPy/RGO, which indicates that the reduction reaction is faster on the composite electrodes than on the pristine PPy electrode.[13,18,30] It could be ascribed to the difference between the morphologies of the composite and the pristine polymer. In comparison with the pristine polymer, the composite can provide larger contact area with the electrolyte and more reactive sites for triiodide reduction because of its porous morphology.[21] Furthermore, the catalytic activity of GO and RGO on reduction of tri-iodide in the composites could also be considered. PPy could act as both the conductive support for GO (RGO) and the catalyst for reduction process. Because of the synergistic effect of PPy and GO or RGO, PPy/GO, and PPy/RGO composite electrodes have shown superior catalytic performance, compared to pristine PPy electrode. Reducing GO in the composite to RGO further enhanced the catalytic performance of the composite on triiodide reduction. This was supposed to due to the improved conductivity of RGO in comparison with that of GO.[37]

According to the above-mentioned CV results, the PPy/RGO electrode fabricated via the two-step electrochemical process could be applied as effective CE for high-performance DSCs. Consequently, the PPy/RGO electrodes with different electro-polymerization time were assembled with TiO_2 photoanode to fabricate DSC devices. The photocurrent density–voltage (J–V) characteristic curves of champion cells are shown in Figure 4a and the corresponding photovoltaic parameters are summarized in Table 1. The statistical data of photovoltaic performance for each group of solar cells with various CEs are presented in Supporting Information Table S1. The electro-polymerization time was finely optimized in terms of the photovoltaic performance. As shown in Figure 4a and Table 1, the open-circuit voltages (V_{oc}) of these devices did not change with the electro-polymerization time, but the short-circuit photocurrent density (J_{sc}) varied slightly. The J_{sc} increased from 14.97 to 15.48 mA cm^{-2} when the polymerization time was prolonged from 100 to 150 s. However, further extension of the polymerization time led to decreased J_{sc}. The devices fabricated with the polymerization time of 200 and 250 s have J_{sc} values of 15.08 and 14.84 mA cm^{-2}, respectively. Fill factor (FF) varied in the same trend as J_{sc} did, with a peak value of 0.60. The initial increase in J_{sc} and FF with polymerization time was possibly due to the increased active area for triiodide reduction on the electrode, which facilitated the charge transfer at the electrolyte/electrode interface. However, too long polymerization time did not improve the active area but just increased the thickness of the film. With the increased thickness of the composite film, the resistance would increase and the diffusion of redox couple in the porous composite film would get more and more difficult, leading to decreased J_{SC} and FF. As a result, the best power conversion efficiency (PCE) of 6.45% was reached at the polymerization time of 150 s with a J_{sc} of 15.48 mA cm^{-2}, a V_{oc} of 0.695 V and a FF of 0.60.

For comparison, the PPy-150 s and PPy/GO-150 s films, and Pt-coated electrode were also applied as CEs in DSCs in the

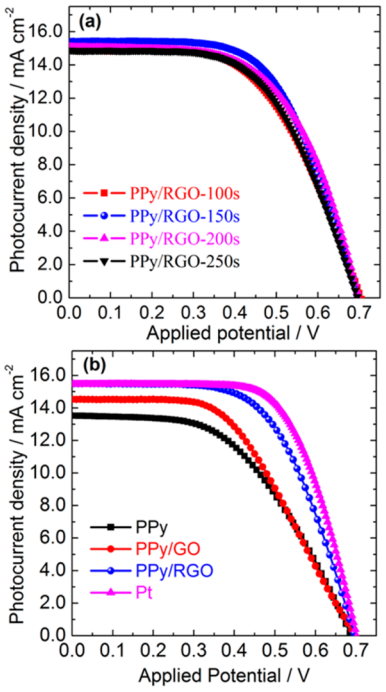

Figure 4. Characteristic photocurrent density–voltage curves of the DSCs containing (a) PPy/RGO CEs prepared with different polymerization time, and (b) PPy, PPy/GO, PPy/RGO, and Pt CEs, measured under solar simulator illumination of 100 mW cm^{-2} (AM 1.5 G).

Table 1. Photovoltaic Parameters of DSCs with Different Counter Electrodes, Measured under Illumination of 100 mW cm^{-2}, AM 1.5 G[a]

counter electrode	V_{oc} (V)	J_{sc} (mA cm^{-2})	FF	PCE (%)
Pt	0.700	15.45	0.66	7.14
PPy	0.685	13.54	0.50	4.64
PPy/RGO-100S	0.695	14.97	0.56	5.83
PPy/RGO-150S	0.695	15.48	0.60	6.45
PPy/GO	0.695	14.28	0.52	5.16
PPy/RGO-200S	0.695	15.08	0.59	6.18
PPy/RGO-250S	0.695	14.84	0.575	5.93

[a] V_{oc} = open-circuit voltage, J_{sc} = short-circuit photocurrent density, FF = fill factor, PCE = power conversion efficiency.

control experiments, and their $J-V$ curves are displayed in Figure 4b, with photovoltaic parameters listed in Table 1. All devices present a similar V_{oc}. As expected, the device based on PPy CE showed the lowest PCE of 4.64% and FF of 0.50, respectively. This was ascribed to the dense microstructure and less active sites of the pristine PPy electrode. After incorporating of GO into PPy film to form PPy/GO composite, the PCE of the device increased to 5.16%, with a J_{sc} of 14.28 mA cm^{-2}, a V_{oc} of 0.695 V, and a FF of 0.52. The improvement of photovoltaic performance can be attributed to the synergetic effect of PPy and GO. When PPy/GO was electrochemically reduced to PPy/RGO, the J_{sc}, and FF of the device improved to 15.48 mA cm^{-2} and 0.60, respectively, resulting in a PCE of 6.45%. The efficiency is comparable with that of the Pt CE-based device (7.14%) with a J_{sc} of 15.45 mA cm^{-2} and a FF of 0.66. The comparable device performance demonstrated that the catalytic ability of the PPy/RGO composites on triiodide reduction is close to that of Pt-based CE, in accordance with the CV results reported in Figure 3. The variation of photovoltaic performance with CEs was confirmed by statistical data reported in Supporting Information Table S1.

Furthermore, the effects of the four CEs, including PPy/GO, PPy/RGO, PPy and Pt on the photovoltaic characteristics of DSCs were investigated using EIS measured under illumination of simulated AM 1.5 G solar light (100 mW cm^{-2}). Nyquist plots of the four devices with various CEs under light illumination are shown in Figure 5 with the equivalent circuit

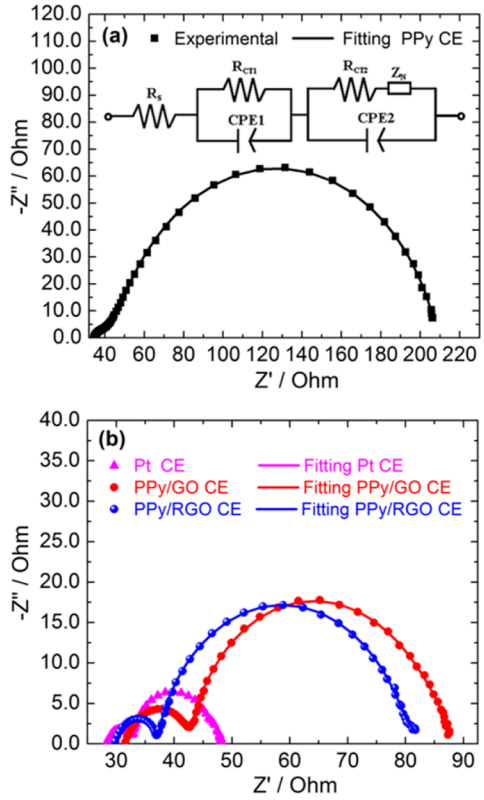

Figure 5. Electrochemical impedance spectra of DSCs using (a) PPy CE and (b) PPy/GO, PPy/RGO, and Pt CEs measured under irradiation of 100 mW cm^{-2} AM 1.5 G at open-circuit voltage; dots present experimental results, and solid lines show fitted results. Inset of panel a shows the equivalent circuit for fitting; the deposition time for PPy-based CE was 150 s.

given as an inset.[38−44] Generally, the EIS of a DSC presents three characteristic semicircles in the scanning frequency range between 10^5 and 0.05 Hz. The high-frequency arc represents the charge-transfer resistance at the interface of the CE/liquid electrolyte (R_{CT1}). The middle-frequency arc is attributed to charge transfer at the TiO_2/dye/electrolyte interfaces (R_{CT2}). The low-frequency arc is ascribed to the Nernst diffusion of the redox couple (I_3^-/I^-) within the electrolyte (Z_N). Additionally, R_S is defined as the substrate resistance, which is mainly related to the sheet resistance of conducting substrate.[39,41] As shown in Figure 5, only two main semicircles are observed for the four devices and the semicircle of Z_N is not obvious and overlapped by R_{CT2} because of the low viscosity of the electrolyte.[39−41] The corresponding fitted values of R_S, R_{CT1}, and R_{CT2} are summarized in Table 2. The value of R_S of four devices is very close, in agreement with the fact that all devices were fabricated under similar conditions. The values for R_{CT1} and R_{CT2} are dependent on the CE used in the devices. The value of

dx.doi.org/10.1021/am5044483 | ACS Appl. Mater. Interfaces 2014, 6, 16249−16256

Table 2. EIS Fitting Parameters of the DSCs with Different Counter Electrodes Measured under Illumination of 100 mW cm^{-2} AM 1.5 G

device	R_S (Ω)	R_{CT1} (Ω)	R_{CT2} (Ω)	R_{TOTAL} (Ω)
PPy	34.40	14.94	160.4	209.74
PPy/GO	31.83	10.79	41.95	84.57
PPy/RGO	30.31	6.59	43.17	80.07
Pt	28.51	4.19	13.98	46.68

R_{CT1} for devices based on PPy, PPy/GO, and PPy/RGO CE is 14.94, 10.79, and 6.59 Ω, respectively. The device with PPy CE also shows the largest R_{CT2} (160.4 Ω). The value of R_{CT2} for devices with PPy/GO and PPy/RGO CEs is 41.95 and 43.17 Ω, respectively. After the introduction of GO and RGO into the polymer, both R_{CT2} and R_{CT1} decrease. According to previous reports,[40,41] R_{CT1} is closely related to the catalytic performance of CE on triiodide reduction. The decrease of R_{CT1} implies the improvement of catalytic performance. The trend of R_{CT1} values is in good agreement with results of CV measurements. The total internal resistance for a DSC device can be expressed as[40]

$$R_{TOTAL} = R_S + R_{CT1} + R_{CT2} + Z_N \quad (1)$$

As the Z_N arc is overlapped by R_{CT2} arc in the study, eq 1 can be described as

$$R_{TOTAL} = R_S + R_{CT1} + R_{CT2} \quad (2)$$

The resistance R_S could be taken as a constant for devices fabricated under the same conditions. The total internal resistance is inversely related to the photovoltaic performance of DSCs.[39−43] The device with Pt CE shows the lowest value of R_{TOTAL} (46.68 Ω) among the four devices, which lead to the highest power conversion efficiency (7.14%). The devices with the PPy-based CE have the largest R_{TOTAL} (209.74 Ω), consistent with its lowest efficiency (4.64%). The incorporation of GO into the polymer CE leads to a significant decrease of R_{TOTAL} of the device to 84.57 Ω. In addition, the reduction of GO to RGO in the composites further decreased R_{TOTAL} to 80.07 Ω. The decrease of R_{TOTAL} helps to improve FF and conversion efficiency of DSC.[39,42,43] As a result, the DSC with PPy/RGO composite CE presents an energy conversion efficiency of 6.45%, which is comparable with that of the device with Pt CE (7.14%). Compared with the pristine polymer (PPy), the composites (PPy/GO and PPy/RGO) can provide larger contact area with the electrolyte and more reactive sites for triiodide reduction because of their porous structures, which could lead to the improvement in the photovoltaic performances for composite-based devices. Reducing GO to RGO in the composites could further enhance the catalytic performance of the composite on triiodide reduction, and thus the photovoltaic performance of device based on PPy/RGO electrode. This could be attributed to the improved conductivity of RGO in comparison with that of GO.

Since the method of preparing PPy/RGO composite film involves no high temperature procedures, it can be readily applied to plastic substrates, such as indium-doped tin oxide coated polyethylene naphthalate (ITO/PEN), which can only sustain temperature lower than 150 °C. The PPy/RGO composite film was prepared successfully on the plastic ITO/PEN substrate using the fabrication parameters optimized for the rigid FTO glass substrate. A photograph of such a composite film on the plastic substrate is shown as an inset of Figure 6. An all-plastic DSC was subsequently assembled

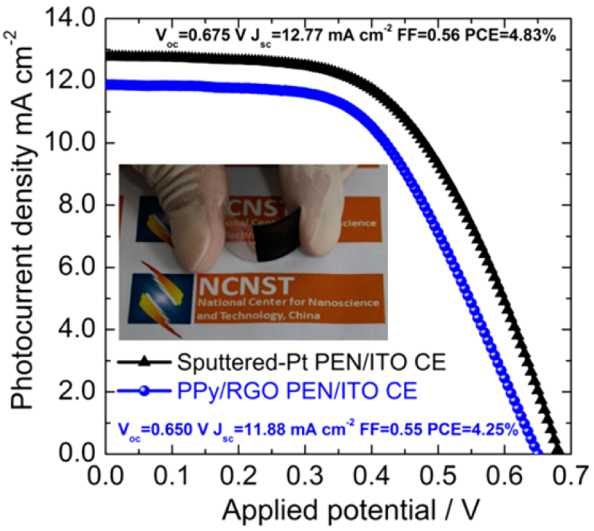

Figure 6. Photovoltaic performances of all-plastic DSCs with plastic PPy/RGO CE and sputtered-Pt CE on ITO/PEN substrate, measured under the irradiation of 100 mW cm^{-2} AM 1.5 G; inset shows the photograph of the plastic PPy/RGO PEN/ITO CE.

with an N719-sensitized P25 TiO_2 electrode as the photoanode and the plastic PPy/RGO composite film as the CE.[45,46] The corresponding current density−voltage curve is presented in Figure 6. The all-plastic DSC device yields an energy conversion efficiency of 4.25% with a V_{oc} of 0.650 V, a J_{sc} of 11.88 mA cm^{-2}, and a FF of 0.55. For comparison, an all plastic DSC with a sputtered Pt ITO/PEN CE was also fabricated. The typical photocurrent density−voltage curve is also plotted in Figure 6. Its photovoltaic parameters are 0.675 V (V_{oc}), 12.77 mA cm^{-2} (J_{sc}), 0.56 (FF), and 4.83% (η), respectively. The all-plastic device with a PPy/RGO composite CE is only slightly inferior to its counterpart with a sputtered Pt CE in photovoltaic performance, indicating that the plastic PPy/RGO composite CE is comparable with the sputtered Pt CE in catalyzing triiodide reduction.

CONCLUSION

In conclusion, high-performance PPy/RGO composite CE for DSCs was fabricated via a two-step electrochemical process at room temperature. CV and EIS results demonstrated that the resultant PPy/RGO composite had a superior catalytic activity toward triiodide reduction. Under the optimized conditions, The DSC with a PPy/RGO composite based CE presented a power conversion efficiency of 6.45%, which is 90% of that of the device using a thermally deposited Pt CE (7.14%). Besides, the all-plastic DSC with PPy/RGO CE exhibited an energy conversion efficiency of 4.25%, which is comparable to the counterpart device with a sputtered-Pt CE in performance (PCE = 4.83%). These results demonstrate that the PPy/RGO composite is a promising alternative to Pt metal to be used as CEs for DSCs. Furthermore, the PPy/RGO composite is prepared at room temperature so it is well suited for plastic devices, which can only sustain temperatures less than 150 °C.

■ ASSOCIATED CONTENT

Supporting Information

Current density−time curves of electrochemical polymerization and reduction, TEM images of PPy and PPy/RGO samples, and statistical data of photovoltaic performance of solar cells with various CEs. This material is available free of charge via the Internet at http://pubs.acs.org.

■ AUTHOR INFORMATION

Corresponding Authors

*E-mail: yinx@nanoctr.cn. Tel: 86-10-8254-5555. Fax: +86-10-62656765

*E-mail: tanggs@mail.buct.edu.cn.

*E-mail: mhe@nanoctr.cn, Tel: +86-10-8254-5555 Fax: +86-10-62656765;

Author Contributions

The manuscript was written through contributions of all authors. All authors have given approval to the final version of the manuscript.

Notes

The authors declare no competing financial interest.

■ ACKNOWLEDGMENTS

This work was financially supported by the National Natural Science Foundation of China (Grant Nos. 21103032 and 51272049) and the Major State Basic Research Development Program of China (973 Program) (No. 2011CB932702).

■ REFERENCES

(1) O'Regan, B.; Gratzel, M. A Low-Cost, High-efficiency Solar Cell Based on Dye-Sensitized Colloidal TiO_2 Films. *Nature* **1991**, *353*, 737−740.

(2) Grätzel, M. Photoelectrochemical Cells. *Nature* **2001**, *414*, 338−344.

(3) Hagfeldt, A.; Boschloo, G.; Sun, L. C.; Kloo, L.; Pettersson, H. Dye-Sensitized Solar Cells. *Chem. Rev.* **2010**, *110*, 6595−6663.

(4) Papageorgiou, N.; Maierand, W. F.; Grätzel, M. An Iodine/Triiodide Reduction Electrocatalyst for Aqueous and Organic Media. *J. Electrochem. Soc.* **1997**, *144*, 876−884.

(5) Hauch, A.; Georg, A. Diffusion in The Electrolyte and Charge-Transfer Reaction at the Platinum Electrode in Dye-sensitized Solar Cells. *Electrochim. Acta* **2001**, *46*, 3457−3466.

(6) Peng, S.; Tian, L.; Liang, J.; Mhaisalkar, S. G.; Ramakrishna, S. Polypyrrole Nanorod Networks/Carbon Nanoparticles Composite Counter Electrodes for High-Efficiency Dye-Sensitized Solar Cells. *ACS Appl. Mater. Interfaces* **2012**, *4*, 397−404.

(7) Peng, T.; Sun, W.; Huang, C.; Yu, W.; Sebo, B.; Dai, Z.; Guo, S.; Zhao, X. Z. Self-Assembled Free-Standing Polypyrrole Nanotube Membrane as an Efficient FTO- and Pt-Free Counter Electrode for Dye-Sensitized Solar Cells. *ACS Appl. Mater. Interfaces* **2014**, *6*, 14−17.

(8) Murakami, T. N.; Grätzel, M. Counter Electrodes for DSC: Application of Functional Materials as Catalysts. *Inorg. Chim. Acta* **2008**, *361*, 572−580.

(9) Wu, J.; Li, Q.; Fan, L.; Lan, Z.; Li, P.; Lin, J.; Hao, S. High-Performance Polypyrrole Nanoparticles Counter Electrode for Dye-Sensitized Solar Cells. *J. Power Sources* **2008**, *181*, 172−176.

(10) Tai, Q.; Chen, B.; Guo, F.; Xu, S.; Hu, H.; Sebo, B.; Zhao, X. Z. In Situ Prepared Transparent Polyaniline Electrode and Its Application in Bifacial Dye-Sensitized Solar Cells. *ACS Nano* **2011**, *5*, 3795−3799.

(11) Sun, H.; Luo, Y.; Zhang, Y.; Li, D.; Yu, Z.; Li, K.; Meng, Q. In Situ Preparation of a Flexible Polyaniline/Carbon Composite Counter Electrode and Its Application in Dye-Sensitized Solar Cells. *J. Phys. Chem. C* **2010**, *114*, 11673−11679.

(12) Chen, J. G.; Wei, H. Y.; Ho, K. C. Using Modified Poly(3,4-Ethylene Dioxythiophene): Poly(Styrene Sulfonate) Film as a Counter Electrode in Dye-Sensitized Solar Cells. *Sol. Energy Mater. Sol. Cells* **2007**, *91*, 1472−1477.

(13) Hong, W.; Xu, Y.; Lu, G.; Li, C.; Shi, G. Transparent graphene/PEDOT−PSS Composite Films as Counter Electrodes of Dye-Sensitized Solar Cells. *Electrochem. Commun.* **2008**, *10*, 1555−1558.

(14) Xu, H.; Zhang, X.; Zhang, C.; Liu, Z.; Zhou, X.; Pang, S.; Chen, X.; Dong, S.; Zhang, Z.; Zhang, L.; Han, P.; Wang, X.; Cui, G. Nanostructured Titanium Nitride/PEDOT:PSS Composite Films as Counter Electrodes of Dye-Sensitized Solar Cells. *ACS Appl. Mater. Interfaces* **2012**, *4*, 1087−1092.

(15) Yin, X.; Wu, F.; Fu, N.; Han, J.; Chen, D.; Xu, P.; He, M.; Lin, Y. Facile Synthesis of Poly(3,4-Ethylenedioxythiophene) Film via Solid-State Polymerization as High-Performance Pt-Free Counter Electrodes for Plastic Dye-Sensitized Solar Cell. *ACS Appl. Mater. Interfaces* **2013**, *5*, 8423−8429.

(16) Murakami, T. N.; Ito, S.; Wang, Q.; Nazeeruddin, M. K.; Bessho, T.; Cesar, I.; Liska, P.; Humphry-Baker, R.; Comte, P.; Péchy, P.; Grätzel, M. Highly Efficient Dye-Sensitized Solar Cells Based on Carbon Black Counter Electrodes. *J. Electrochem. Soc.* **2006**, *153*, A2255−A2261.

(17) Dong, P.; Pint, C.; Mirri, F.; Zhan, Y. J.; Zhang, J.; Pasquali, M.; Hauge, R.; Verduzco, R.; Jiang, M.; Lin, H.; Lou, J. Vertically Aligned Single-Walled Carbon Nanotubes as Low-Cost and High Electrocatalytic Counter Electrode for Dye-Sensitized Solar Cells. *ACS Appl. Mater. Interfaces* **2011**, *3*, 3157−3161.

(18) Lee, W. J.; Ramasamy, E.; Lee, D. Y.; Song, J. S. Efficient Dye-Sensitized Cells with Catalytic Multiwall Carbon Nanotube Counter Electrodes. *ACS Appl. Mater. Interfaces* **2009**, *1*, 1145−1149.

(19) Roy-mayhew, J. D.; Bozym, D. J.; Punckt, C.; Aksay, I. A. Functionalized Graphene as a Catalytic Counter Electrode in Dye-Sensitized Solar Cells. *ACS Nano* **2010**, *4*, 6203−6211.

(20) Kavan, L.; Yum, J. H.; Grätzel, M. Optically Transparent Cathode for Dye-Sensitized Solar Cells Based on Graphene Nanoplatelets. *ACS Nano* **2011**, *5*, 165−172.

(21) Roy-Mayhew, J. D.; Aksay, I. A. Graphene Materials and Their Use in Dye-Sensitized Solar Cells. *Chem. Rev.* **2014**, *114*, 6323−6348.

(22) Hasin, P.; Alpuche-Aviles, M. A.; Wu, Y. Y. Electrocatalytic Activity of Graphene Multilayers toward I^-/I_3^-: Effect of Preparation Conditions and Polyelectrolyte Modification. *J. Phys. Chem. C* **2010**, *114*, 15857−15861.

(23) Zheng, H.; Neo, C. Y.; Ouyang, J. Highly Efficient Iodide/Triiodide Dye-Sensitized Solar Cells with Gel-Coated Reduce Graphene Oxide/Single-Walled Carbon Nanotube Composites as the Counter Electrode Exhibiting an Open-Circuit Voltage of 0.90 V. *ACS Appl. Mater. Interfaces* **2013**, *5*, 6657−6664.

(24) Li, Z.; Gong, F.; Zhou, G.; Wang, Z. S. NiS_2/Reduced Graphene Oxide Nanocomposites for Efficient Dye-Sensitized Solar Cells. *J. Phys. Chem. C* **2013**, *117*, 6561−6566.

(25) Ramanavičius, A.; Ramanavičienė, A.; Malinauskas, A. Electrochemical Sensors Based on Conducting Polymer−Polypyrrole. *Electrochim. Acta* **2006**, *51*, 6025−6037.

(26) Deronzier, A.; Moutet, J. C. Polypyrrole Films Containing Metal Complexes: Syntheses and Applications. *Coord. Chem. Rev.* **1996**, *147*, 339−371.

(27) Liang, M.; Wang, J.; Luo, B.; Qiu, T.; Zhi, L. High-Efficiency and Room-Temperature Reduction of Graphene Oxide: A Facile Green Approach Towards Flexible Graphene Films. *Small* **2012**, *8*, 1180−1184.

(28) Chen, D.; Feng, H.; Li, J. Graphene Oxide: Preparation, Functionalization, and Electrochemical Applications. *Chem. Rev.* **2012**, *112*, 6027−6053.

(29) Yen, M. Y.; Teng, C. C.; Hsiao, M. C.; Liu, P. I.; Chuang, W. P.; Ma, C. C. M.; Hsieh, C. K.; Tsai, M. C.; Tsai, C. H. Platinum Nanoparticles/Graphene Composite Catalyst as a Novel Composite Counter Electrode for High Performance Dye-Sensitized Solar Cells. *J. Mater. Chem.* **2011**, *21*, 12880−12888.

(30) Xue, Y.; Liu, J.; Chen, H.; Wang, R.; Li, D.; Qu, J.; Dai, L. Nitrogen-Doped Graphene Foams as Metal-Free Counter Electrodes

in High-Performance Dye-Sensitized Solar Cells. *Angew. Chem., Int. Ed.* **2012**, *51*, 12124−12127.
(31) Chen, L.; Guo, C. X.; Zhang, Q.; Lei, Y.; Xie, J.; Ee, S.; Guai, G.; Song, Q.; Li, C. M. Graphene Quantum-Dot-Doped Polypyrrole Counter Electrode for High-Performance Dye-Sensitized Solar Cells. *ACS Appl. Mater. Interfaces* **2013**, *5*, 2047−2052.
(32) Gong, F.; Xu, X.; Zhou, G.; Wang, Z. S. Enhanced Charge Transportation in A Polypyrrole Counter Electrode via Incorporation of Reduced Graphene Oxide Sheets for Dye-sensitized Solar Cells. *Phys. Chem. Chem. Phys.* **2013**, *15*, 546−552.
(33) Hummers, W. S.; Offeman, R. E. Preparation of Graphitic Oxide. *J. Am. Chem. Soc.* **1958**, *80*, 1339−1339.
(34) Shao, Y.; Wang, J.; Engelhard, M.; Wang, C.; Lin, Y. Facile and Controllable Electrochemical Reduction of Graphene Oxide and Its Applications. *J. Mater. Chem.* **2010**, *20*, 743−748.
(35) Wang, Z.; Zhou, X.; Zhang, J.; Boey, F.; Zhang, H. Direct Electrochemical Reduction of Single-Layer Graphene Oxide and Subsequent Functionalization with Glucose Oxidase. *J. Phys. Chem. C* **2009**, *113*, 14071−14075.
(36) Li, X.; Wang, H.; Robinson, J. T.; Sanchez, H.; Diankov, G.; Dai, H. Simultaneous Nitrogen Doping and Reduction of Graphene Oxide. *J. Am. Chem. Soc.* **2009**, *131*, 15939−15944.
(37) Yang, Y.; Wang, C.; Yue, B.; Gambhir, S.; Too, C. O.; Wallace, G. G. Electrochemically Synthesized Polypyrrole/Graphene Composite Film for Lithium Batteries. *Adv. Energy Mater.* **2012**, *2*, 266−272.
(38) Trevisan, R.; Döbbelin, M.; Boix, P. P.; Barea, E. M.; Tena-Zaera, R.; Mora-Seró, I.; Bisquert, J. PEDOT Nanotube Arrays as High Performing Counter Electrodes for Dye Sensitized Solar Cells. Study of the Interactions among Electrolytes and Counter Electrodes. *Adv. Energy Mater.* **2011**, *1*, 781−784.
(39) Han, L.; Koide, N.; Chiba, Y.; Mitate, T. Modeling of An Equivalent Circuit for Dye-Sensitized Solar Cells. *Appl. Phys. Lett.* **2004**, *84*, 2433−2435.
(40) Han, L.; Koide, N.; Chiba, Y.; Islam, A.; Komiya, R.; Fuke, N.; Fukui, A.; Yamanaka, R. Improvement of Efficiency of Dye-sensitized Solar Cells by Reduction of Internal Resistance. *Appl. Phys. Lett.* **2005**, *86*, No. 213501.
(41) Fabregat-Santiago, F.; Bisquert, J.; Palomares, E.; Otero, L.; Kuang, D.; Zakeeruddin, S. M.; Grätzel, M. Correlation between Photovoltaic Performance and Impedance Spectroscopy of Dye-Sensitized Solar Cells Based on Ionic Liquids. *J. Phys. Chem. C* **2007**, *111*, 6550−6560.
(42) Fu, N.; Xiao, X.; Zhou, X.; Zhang, J.; Lin, Y. Electrodeposition of Platinum on Plastic Substrates as Counter Electrodes for Flexible Dye-Sensitized Solar Cells. *J. Phys. Chem. C* **2012**, *116*, 2850−2857.
(43) Yin, X.; Xue, Z.; Liu, B. Electrophoretic Deposition of Pt Nanoparticles on Plastic Substrates as Counter Electrode for Flexible Dye-Sensitized Solar Cells. *J. Power Sources* **2011**, *196*, 2422−2426.
(44) Yin, X.; Wang, B.; He, M.; He, T. Facile Synthesis of ZnO Nanocrystals via a Solid State Reaction for High Performance Plastic Dye-Sensitized Solar Cells. *Nano Res.* **2012**, *5*, 1−10.
(45) Yin, X.; Xue, Z.; Wang, L.; Cheng, Y.; Liu, B. High-Performance Plastic Dye-Sensitized Solar Cells Based on Low-Cost Commercial P25 TiO_2 and Organic Dye. *ACS Appl. Mater. Interfaces* **2012**, *4*, 1709−1715.
(46) Weerasinghe, H. C.; Huang, F. Z.; Cheng, Y.-B. Fabrication of Flexible Dye Sensitized Solar Cells On Plastic Substrates. *Nano Energy* **2013**, *2*, 174−189.